

## Supplementary Information

# Zwitterion-derived ligand-coated ZnO Quantum Dots Engineered via an Organometallic Approach

Zygmunt Drużyński,<sup>[a]</sup> Małgorzata Wolska-Pietkiewicz,<sup>\*[a]</sup> Janusz Lewiński<sup>\*[a,b]</sup>

<sup>a</sup> Faculty of Chemistry, Warsaw University of Technology, Noakowskiego 3, Warsaw 00-664, Poland

<sup>b</sup> Institute of Physical Chemistry, Polish Academy of Sciences, Kasprzaka 44/52, Warsaw 01-224, Poland

## Table of contents:

<b>Characterization of zwitterionic-type ligand-coated ZnO QDs</b> .....	2
1. High-resolution transmission electron microscopy (HRTEM).....	2
2. Powder X-ray diffraction (PXRD).....	3
3. Dynamic light scattering (DLS) analysis.....	5
4. Thermogravimetric analysis (TGA).....	7
5. Optical parameters.....	8
<b>Solubility and stability of ligand-coated ZnO QDs</b> .....	12
1. Solution stability of ZnO QDs coated with zwitterion-derived ligands.....	12
2. Solution stability of ZnO QDs coated with carboxylate ligands.....	16
3. Effect of buffer pH and water on the colloidal stability and luminescence of ZnO-BET QDs.....	18

# Characterization of zwitterionic-type ligand-coated ZnO QDs

## 1. High-resolution transmission electron microscopy (HRTEM)

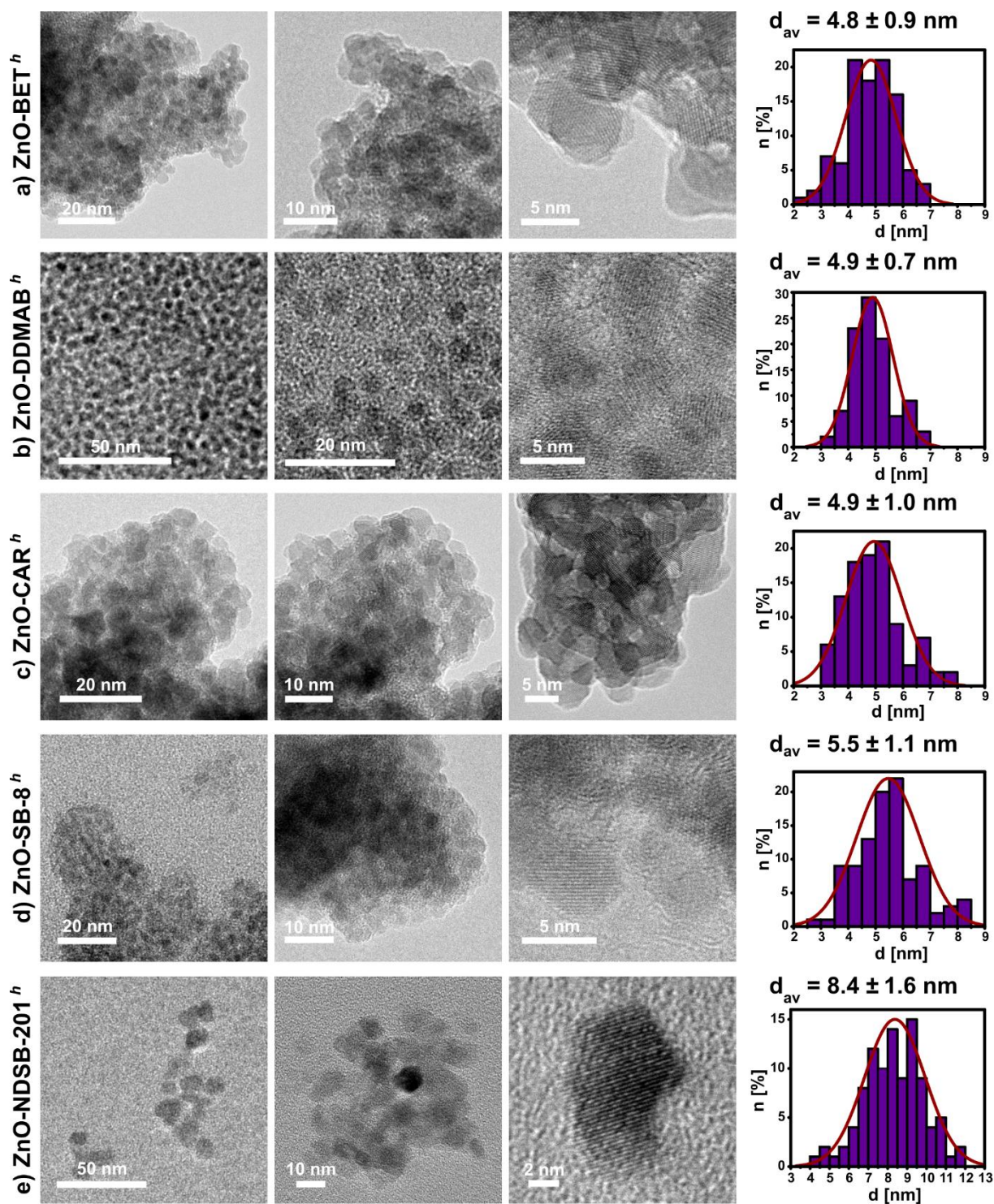


Figure S1. Representative HRTEM micrographs of ZnO-X<sup>h</sup> QDs along with their size distributions and Gaussian approximation.

## 2. Powder X-ray diffraction (PXRD)

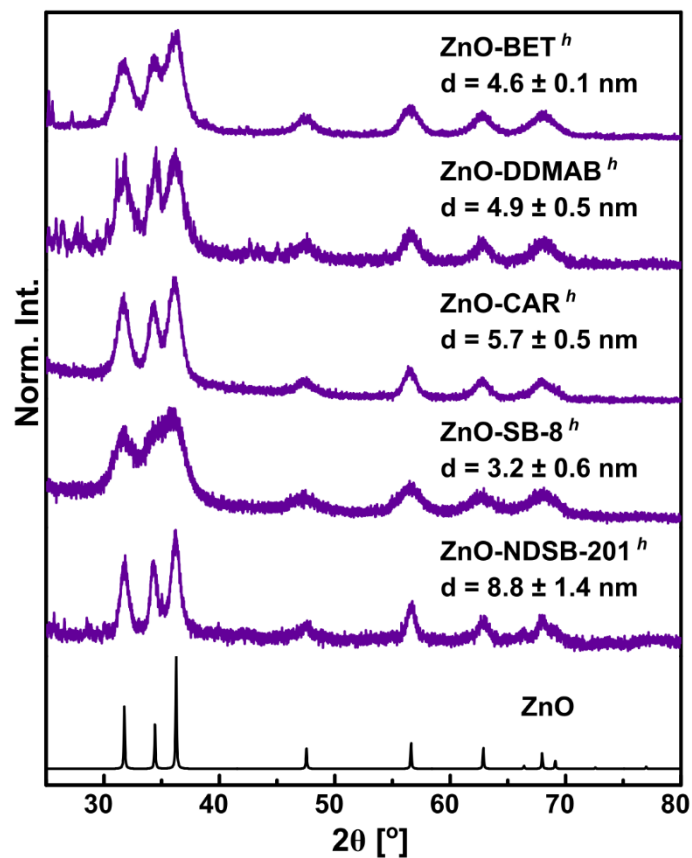


Figure S2. The powder X-ray diffraction patterns of ZnO-X<sup>h</sup> QDs with estimation of nanocrystal sizes using the Scherrer equation.

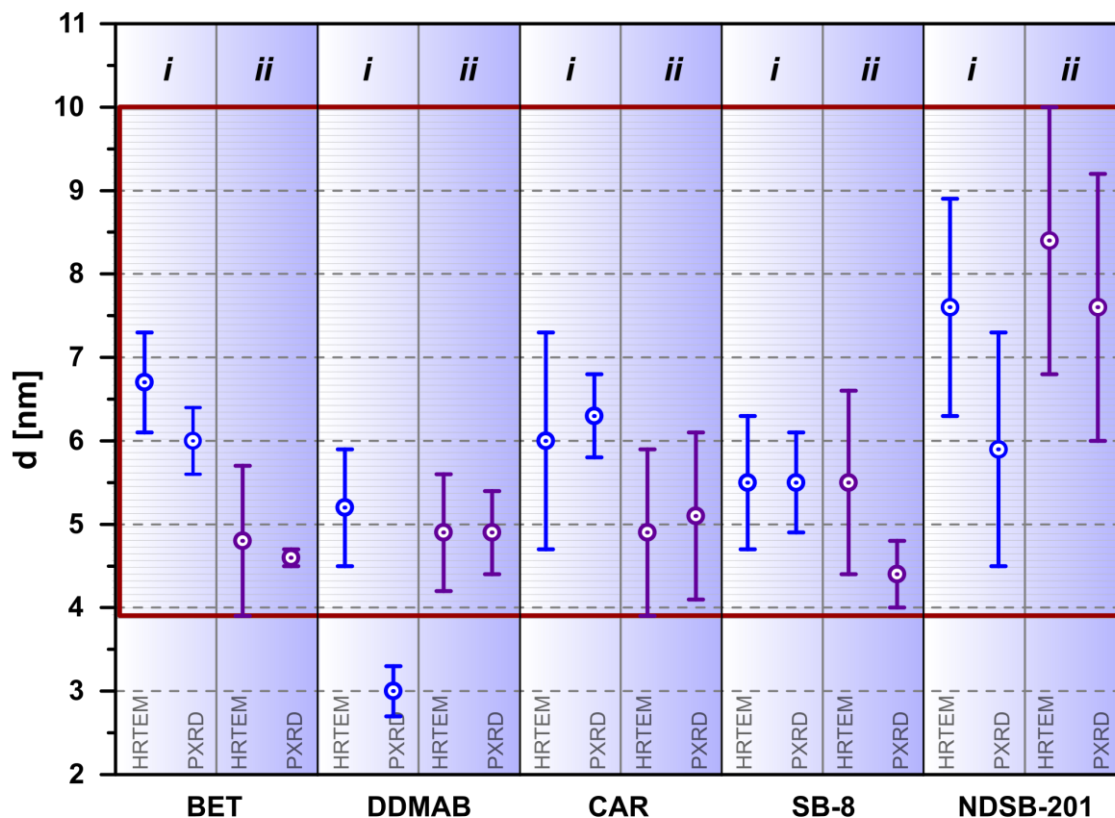
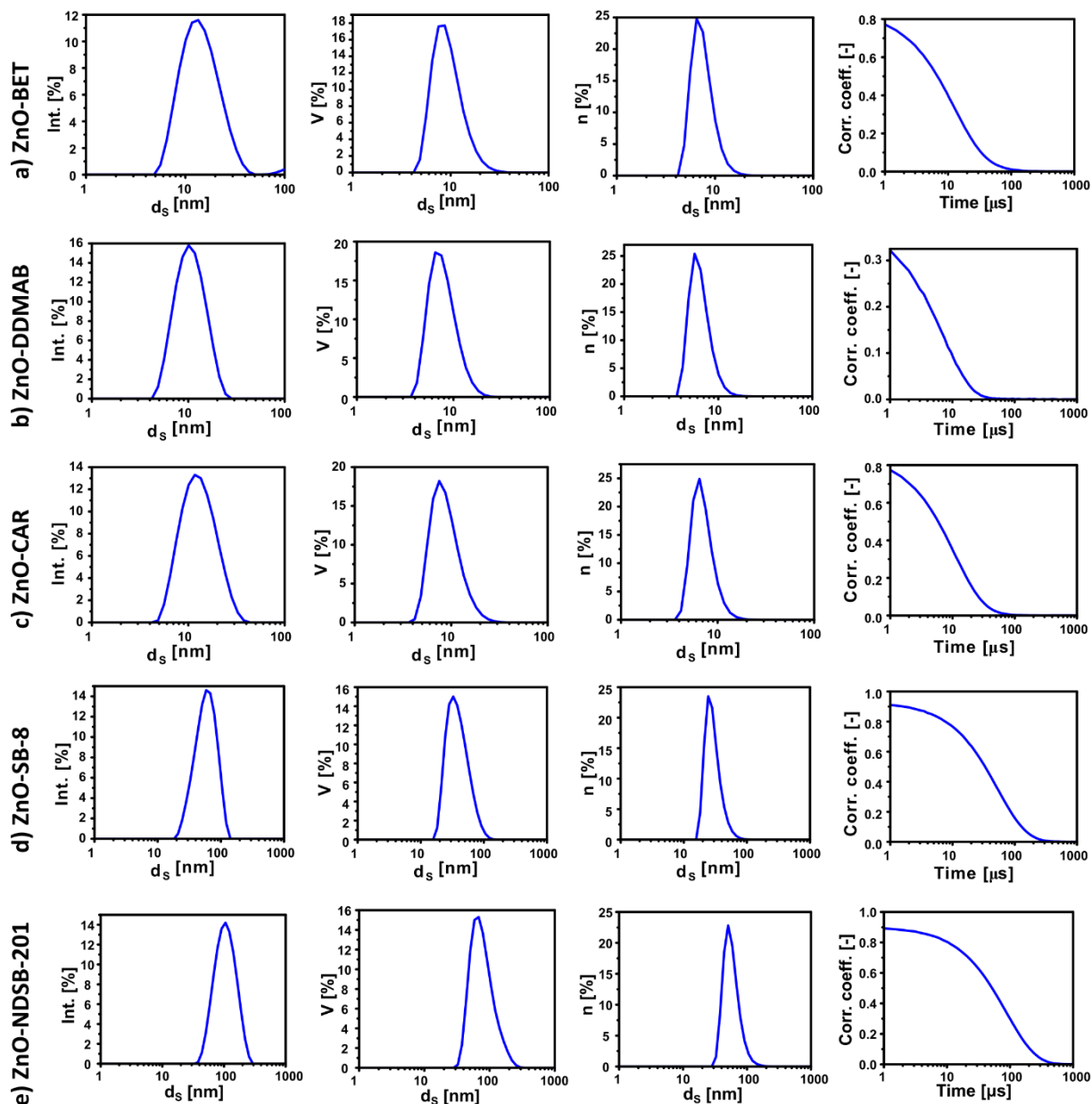


Figure S3. The representation of the core sizes of ZnO QDs derived from HRTEM and PXRD data, with an additional marked range containing sizes with a standard deviation from HRTEM.

**Tab. S1.** Comparison of ZnO QD core diameters as determined from HRTEM micrographs and calculated via the Scherrer formula from PXRD diffractograms, for two distinct synthesis methods.

QDs	approach	Inorganic core diameter of ZnO QDs [nm]	
		HRTEM	PXRD
ZnO-BET	<i>i</i>	6.7 ± 0.6	6.0 ± 0.4
ZnO-BET <sup>h</sup>	<i>ii</i>	4.8 ± 0.9	4.6 ± 0.1
ZnO-DDMAB	<i>i</i>	5.2 ± 0.7	3.0 ± 0.3
ZnO-DDMAB <sup>h</sup>	<i>ii</i>	4.9 ± 0.7	4.9 ± 0.5
ZnO-CAR	<i>i</i>	6.0 ± 1.3	6.3 ± 0.5
ZnO-CAR <sup>h</sup>	<i>ii</i>	4.9 ± 1.0	5.1 ± 1.0
ZnO-SB-8	<i>i</i>	5.5 ± 0.8	5.5 ± 0.6
ZnO-SB-8 <sup>h</sup>	<i>ii</i>	5.5 ± 1.1	4.4 ± 0.4
ZnO-NDSB-201	<i>i</i>	7.6 ± 1.3	5.9 ± 1.4
ZnO-NDSB-201 <sup>h</sup>	<i>ii</i>	8.4 ± 1.6	7.6 ± 1.6

### 3. Dynamic light scattering (DLS) analysis



**Figure S4.** Intensity-, volume-, and number-averaged size distribution of solvodynamic diameter of zwitterion-derived ligand-coated ZnO QDs obtained from the representative DLS measurements: in methanol for **ZnO-BET**, **ZnO-CAR**, **ZnO-SB-8**, **ZnO-NDSB-201** QDs; and in toluene for **ZnO-DDMAB** QDs. Correlation coefficients are shown as a function of time.

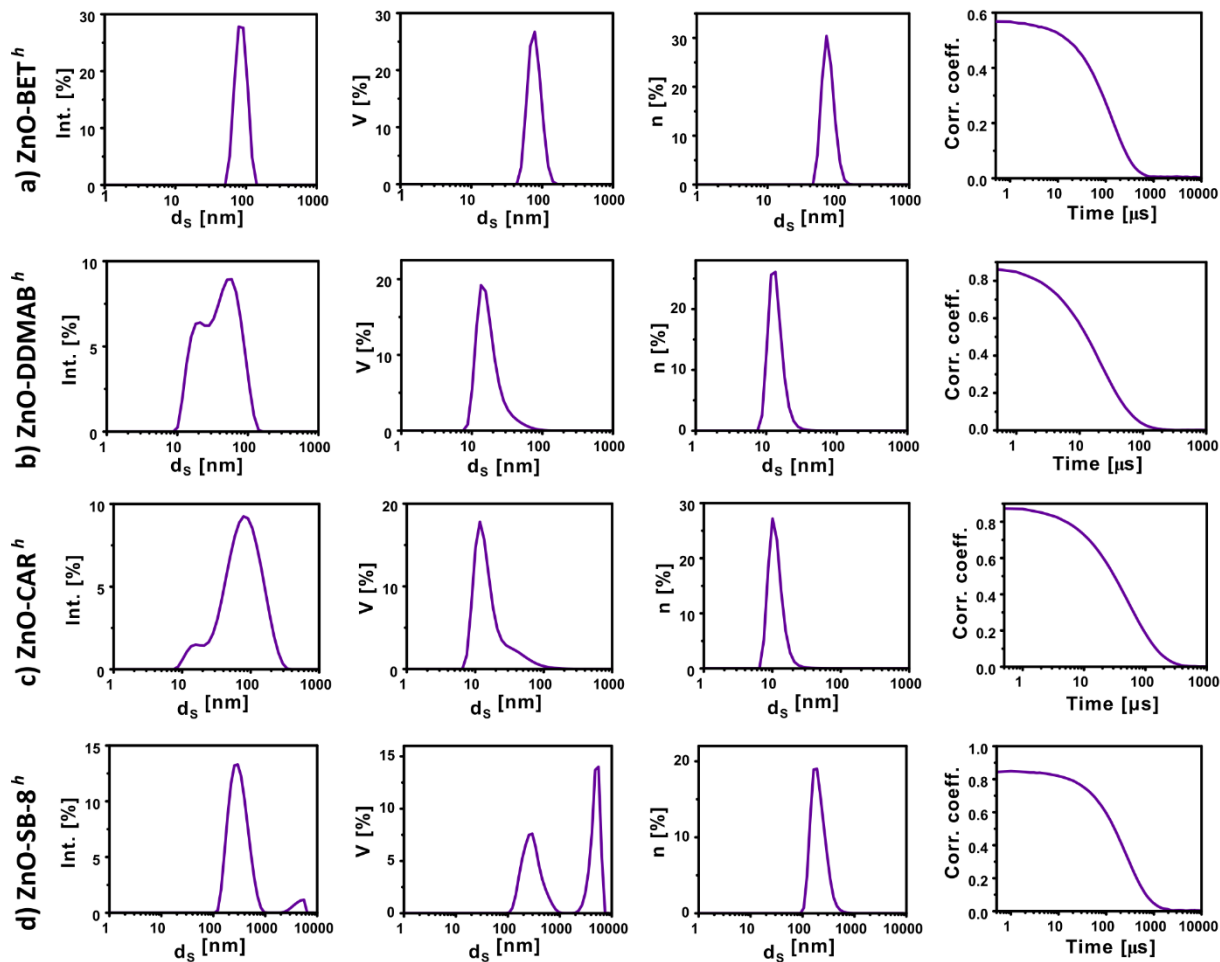


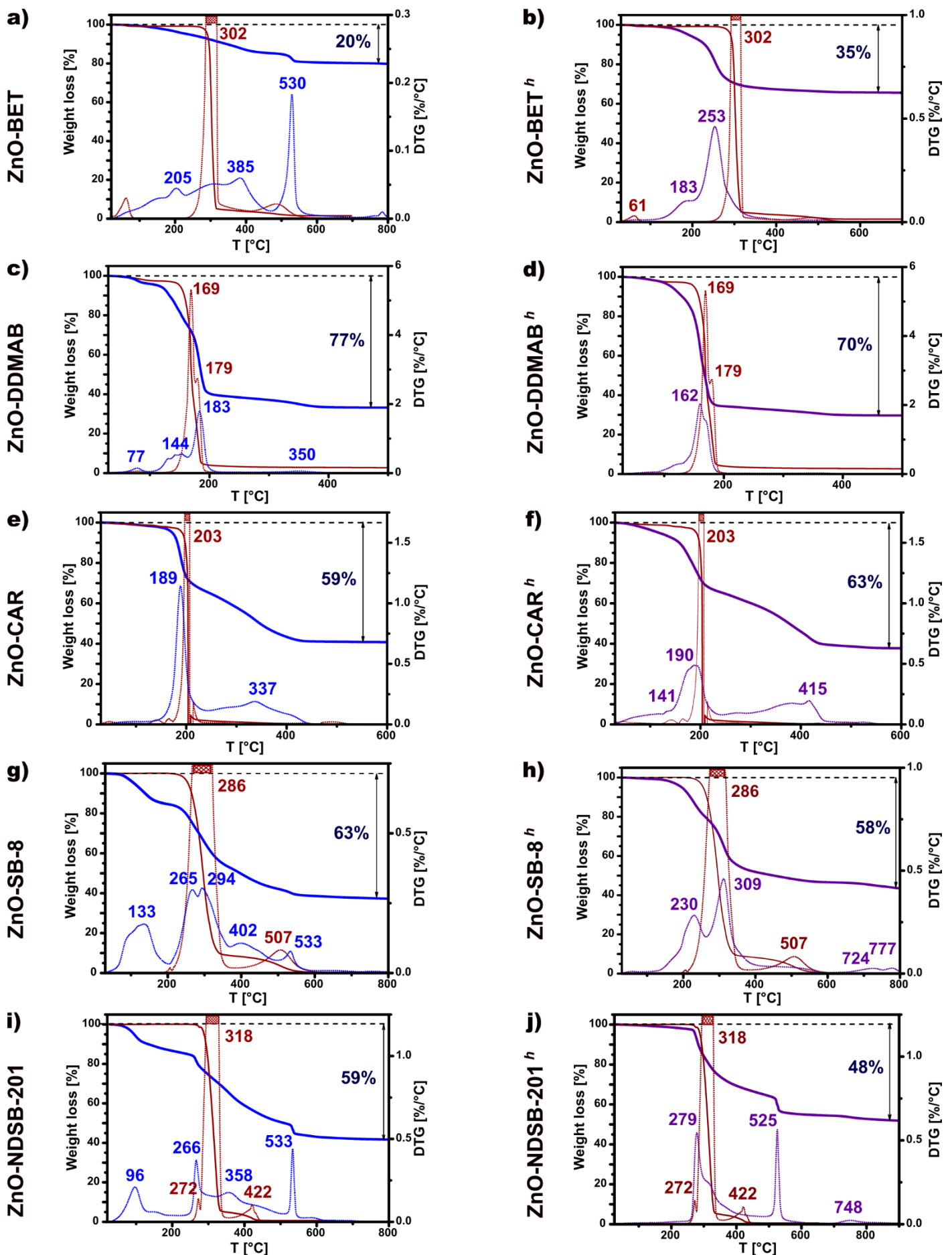
**Figure S5.** Intensity-, volume-, and number-averaged size distribution of solvodynamic diameter of zwitterion-derived ligand-coated ZnO QDs obtained from the representative DLS measurements: in methanol for **ZnO-CAR<sup>h</sup>**, **ZnO-SB-8<sup>h</sup>** QDs, in ethanol for **ZnO-BET<sup>h</sup>** QDs; and in THF for **ZnO-DDMAB<sup>h</sup>** QDs. Correlation coefficients are shown as a function of time.

**Tab. S2.** Solvodynamic diameters of zwitterion-capped ZnO QDs obtained from the representative DLS measurements presented in **Figures S4-S5**, also derived from the intensity-, volume-, and number-mode, and additionally Z-av values (italic font) obtained from measurements for other dispersions not included in **Figures S4, S5**, and **Table 1**.

QDs	Z-av [nm] (PDI)	Int. [nm]	V. [nm]	n [nm]
<b>ZnO-BET</b>	14.5 (0.251) <sup>3</sup>	15.5 ± 7.2	9.6 ± 3.8	7.5 ± 2.1
<b>ZnO-BET<sup>h</sup></b>	114.6 (0.103) <sup>4</sup>	128.9 ± 43.9	105.5 ± 42.1	77.9 ± 24.1
<b>ZnO-DDMAB</b>	9.9 (0.129) <sup>2</sup>	11.6 ± 4.7	7.4 ± 2.9	5.6 ± 1.7
<b>ZnO-DDMAB<sup>h</sup></b>	14.8 (0.173) <sup>1</sup>	16.7 ± 6.8	11.2 ± 4.2	8.8 ± 2.4
<b>ZnO-CAR</b>	12.2 (0.178) <sup>3</sup>	13.7 ± 5.7	9.1 ± 3.4	7.1 ± 2.0
<b>ZnO-CAR<sup>h</sup></b>	59.6 (0.284) <sup>3</sup>	90.9 ± 50.9	19.1 ± 17.3	11.5 ± 3.4
<b>ZnO-SB-8</b>	36.0 (0.269) <sup>3</sup>	51.0 ± 32.4	13.5 ± 10.3	7.8 ± 2.6
<b>ZnO-SB-8<sup>h</sup></b>	299.8 (0.205) <sup>3</sup>	323.0 ± 130.5	310.6 ± 135.5	212.3 ± 74.4
<b>ZnO-NDSB-201</b>	95.5 (0.132) <sup>3</sup>	111.4 ± 42.5	81.8 ± 36.0	58.5 ± 18.6
<b>ZnO-NDSB-201<sup>h</sup></b>		n.d.		

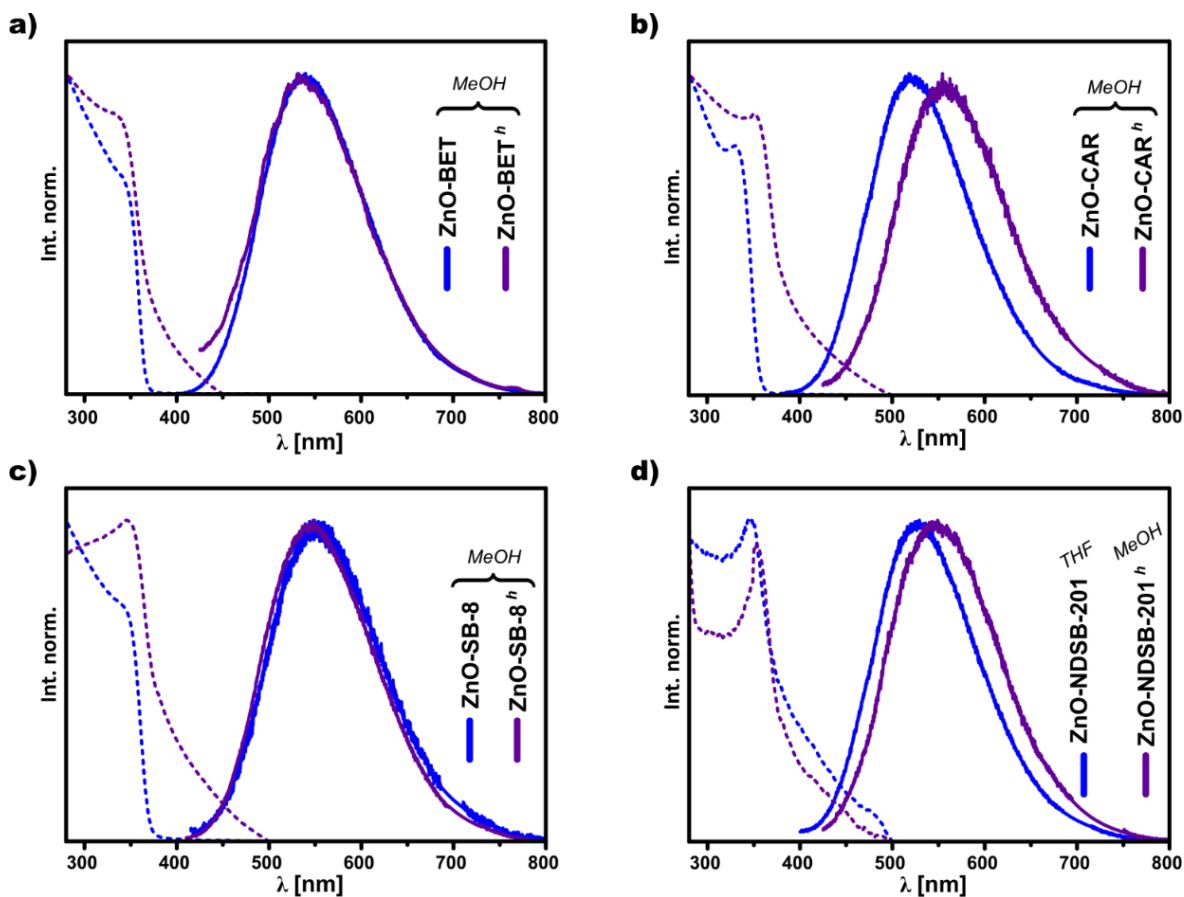
Abbreviations: <sup>1</sup> – THF, <sup>2</sup> – DMSO, <sup>3</sup> – methanol, <sup>4</sup> – ethanol

#### 4. Thermogravimetric analysis (TGA)



**Figure S6.** Results of thermogravimetric analysis for all ZnO QDs (weight loss [%] (solid line) and its derivative [%/°C] (dotted line)). Each diagram is supplemented with the result of the TGA for the proper pro-ligand, i.e., pure (sulfo)betaine compound (respectively, red and red dotted line).

## 5. Optical parameters

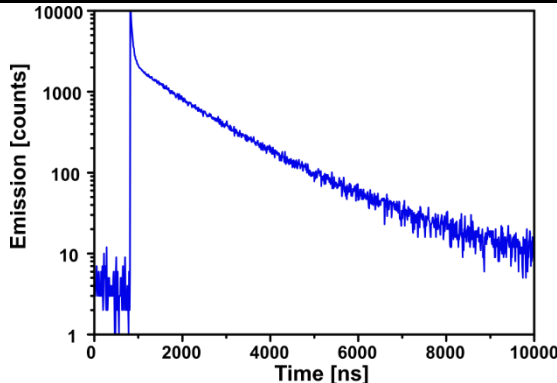
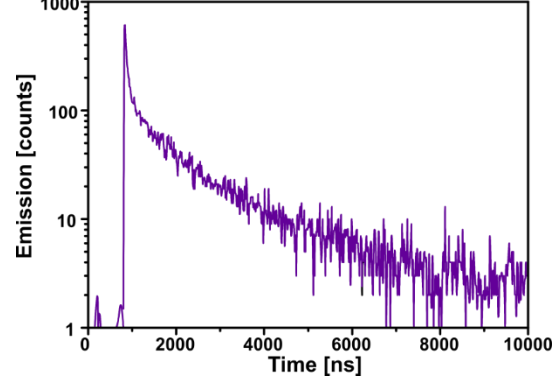


**Figure S7.** Absorption (dotted line) and emission (solid line) spectra of ZnO QDs in methanol or THF dispersion.

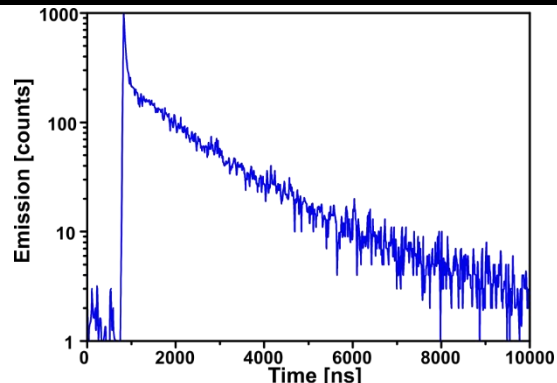
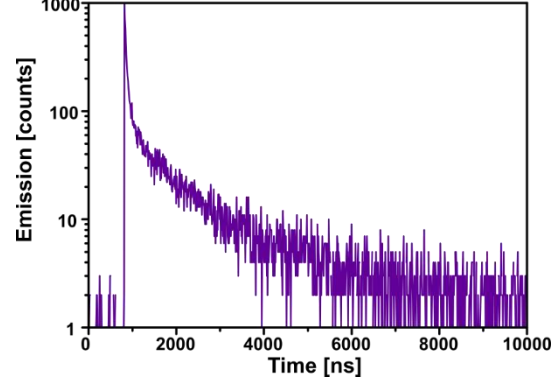
**Tab. S3.** Fluorescence lifetime components ( $\tau_{1-3}$ ) with contributions and  $\langle\tau\rangle$ ,  $\chi^2$  from 3<sup>rd</sup> exponential fitting to exponential decay of PL for ZnO QDs stabilized by betaine ( $\lambda_{\text{ex}} = 340$  nm).

QDs	$\tau$ [ns] (contrib. %)	PL decay
ZnO-BET [Error! Bookmark not defined.]	$\tau_1 = 49.3$ (81)	
	$\tau_2 = 1150.3$ (13)	
	$\tau_3 = 3619.5$ (6)	
	$\langle\tau\rangle = 2304.0$	
	$\chi^2 = 1.15$	
ZnO-BET <sup>h</sup>	$\tau_1 = 24.3$ (92)	
	$\tau_2 = 268.4$ (6)	
	$\tau_3 = 1582.9$ (2)	
	$\langle\tau\rangle = 718.3$	
	$\chi^2 = 1.57$	

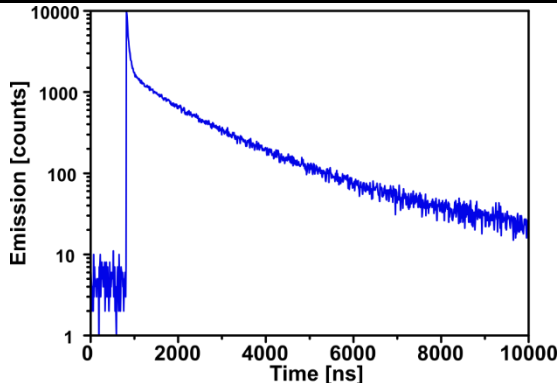
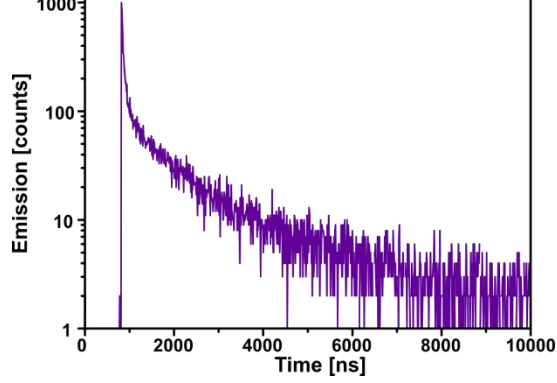
**Tab. S4.** Fluorescence lifetime components ( $\tau_{1-3}$ ) with contributions and  $\langle\tau\rangle$ ,  $\chi^2$  from 3<sup>rd</sup> exponential fitting to exponential decay of PL for ZnO QDs stabilized by DDMAB ( $\lambda_{\text{ex}} = 340$  nm).

QDs	$\tau$ [ns] (contrib. %)	PL decay
ZnO-DDMAB	$\tau_1 = 42.2$ (82)	
	$\tau_2 = 783.2$ (9)	
	$\tau_3 = 1641.8$ (9)	
	$\langle\tau\rangle = 1169.4$	
	$\chi^2 = 1.15$	
ZnO-DDMAB <sup>h</sup>	$\tau_1 = 28.7$ (88)	
	$\tau_2 = 473.0$ (8)	
	$\tau_3 = 1486.2$ (4)	
	$\langle\tau\rangle = 867.3$	
	$\chi^2 = 1.25$	

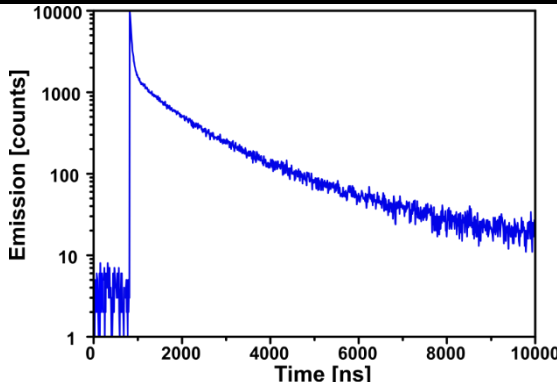
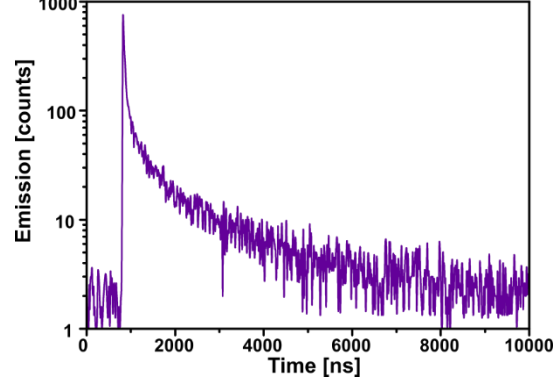
**Tab. S5.** Fluorescence lifetime components ( $\tau_{1-3}$ ) with contributions and  $\langle\tau\rangle$ ,  $\chi^2$  from 3<sup>rd</sup> exponential fitting to exponential decay of PL for ZnO QDs stabilized by L-carnitine ( $\lambda_{\text{ex}} = 340$  nm).

QDs	$\tau$ [ns] (contrib. %)	PL decay
ZnO-CAR	$\tau_1 = 44.8$ (82)	
	$\tau_2 = 966.0$ (9)	
	$\tau_3 = 2030.9$ (9)	
	$\langle\tau\rangle = 1464.6$	
	$\chi^2 = 1.10$	
ZnO-CAR <sup>h</sup>	$\tau_1 = 27.9$ (84)	
	$\tau_2 = 124.8$ (11)	
	$\tau_3 = 1103.6$ (5)	
	$\langle\tau\rangle = 656.2$	
	$\chi^2 = 0.92$	

**Tab. S6.** Fluorescence lifetime components ( $\tau_{1-3}$ ) with contributions and  $\langle\tau\rangle$ ,  $\chi^2$  from 3<sup>rd</sup> exponential fitting to exponential decay of PL for ZnO QDs stabilized by SB-8 ( $\lambda_{\text{ex}} = 340$  nm).

QDs	$\tau$ [ns] (contrib. %)	PL decay
ZnO-SB-8	$\tau_1 = 42.5$ (86)	
	$\tau_2 = 857.1$ (10)	
	$\tau_3 = 2522.9$ (4)	
	$\langle\tau\rangle = 1508.3$	
	$\chi^2 = 1.21$	
ZnO-SB-8 <sup>h</sup>	$\tau_1 = 33.3$ (88)	
	$\tau_2 = 724.6$ (9)	
	$\tau_3 = 2484.9$ (3)	
	$\langle\tau\rangle = 1363.2$	
	$\chi^2 = 1.26$	

**Tab. S7.** Fluorescence lifetime components ( $\tau_{1-3}$ ) with contributions and  $\langle\tau\rangle$ ,  $\chi^2$  from 3<sup>rd</sup> exponential fitting to exponential decay of PL for ZnO QDs stabilized by NDSB-201 ( $\lambda_{\text{ex}} = 340$  nm).

QDs	$\tau$ [ns] (contrib. %)	PL decay
ZnO-NDSB-201	$\tau_1 = 39.8$ (86)	
	$\tau_2 = 731.0$ (11)	
	$\tau_3 = 2487.0$ (3)	
	$\langle\tau\rangle = 1336.4$	
	$\chi^2 = 1.28$	
ZnO-NDSB-201 <sup>h</sup>	$\tau_1 = 28.8$ (89)	
	$\tau_2 = 198.8$ (8)	
	$\tau_3 = 1289.6$ (3)	
	$\langle\tau\rangle = 680.7$	
	$\chi^2 = 1.02$	

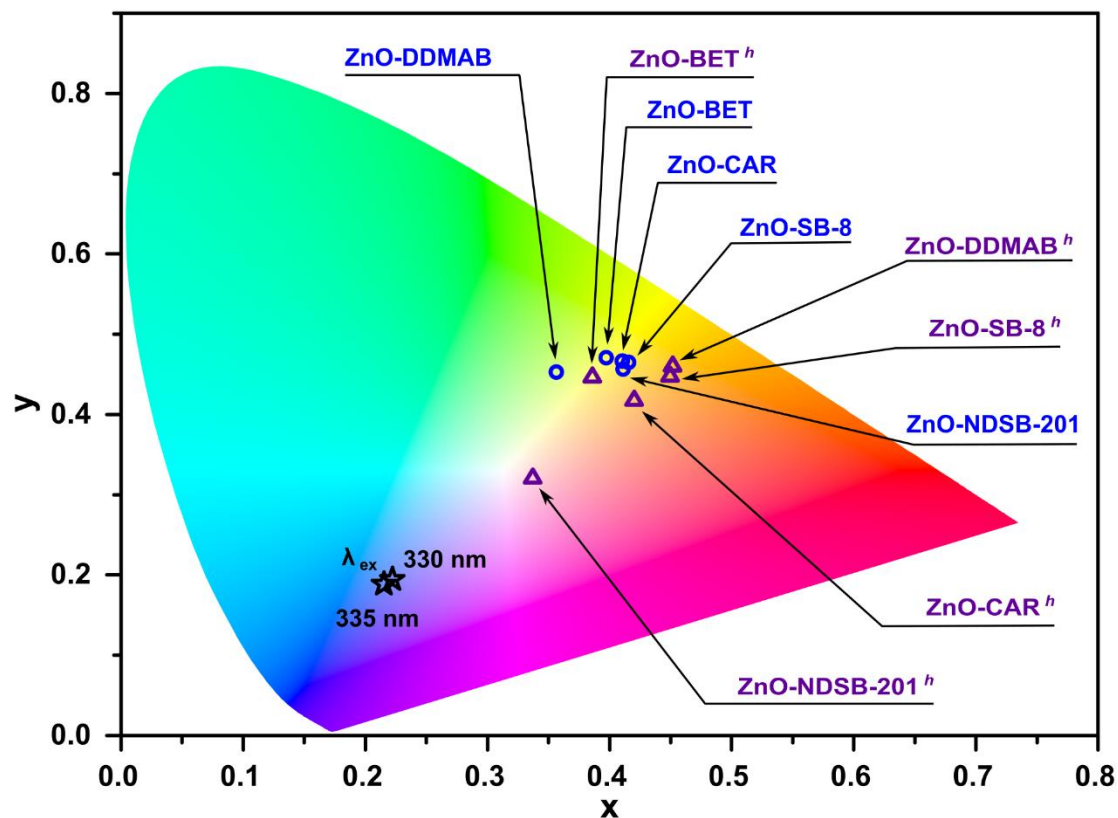


**Figure S8.** Chromaticity colour coordinates in CIE diagrams of the: **ZnO-BET** [0.3975, 0.4703], **ZnO-BET<sup>h</sup>** [0.3861, 0.4461], **ZnO-DDMAB** [0.3565, 0.4528], **ZnO-DDMAB<sup>h</sup>** [0.4516, 0.4599], **ZnO-CAR** [0.4106, 0.4661], **ZnO-CAR<sup>h</sup>** [0.4202, 0.4173], **ZnO-SB-8** [0.4157, 0.4648], **ZnO-SB-8<sup>h</sup>** [0.4498, 0.4472], **ZnO-NDSB-201** [0.4111, 0.4562], and **ZnO-NDSB-201<sup>h</sup>** [0.3371, 0.3204] QDs, obtained by *i* (blue circles) or *ii* (violet triangles) synthetic method.

# Solubility and stability of ligand-coated ZnO QDs

## 1. Solution stability of ZnO QDs coated with zwitterion-derived ligands

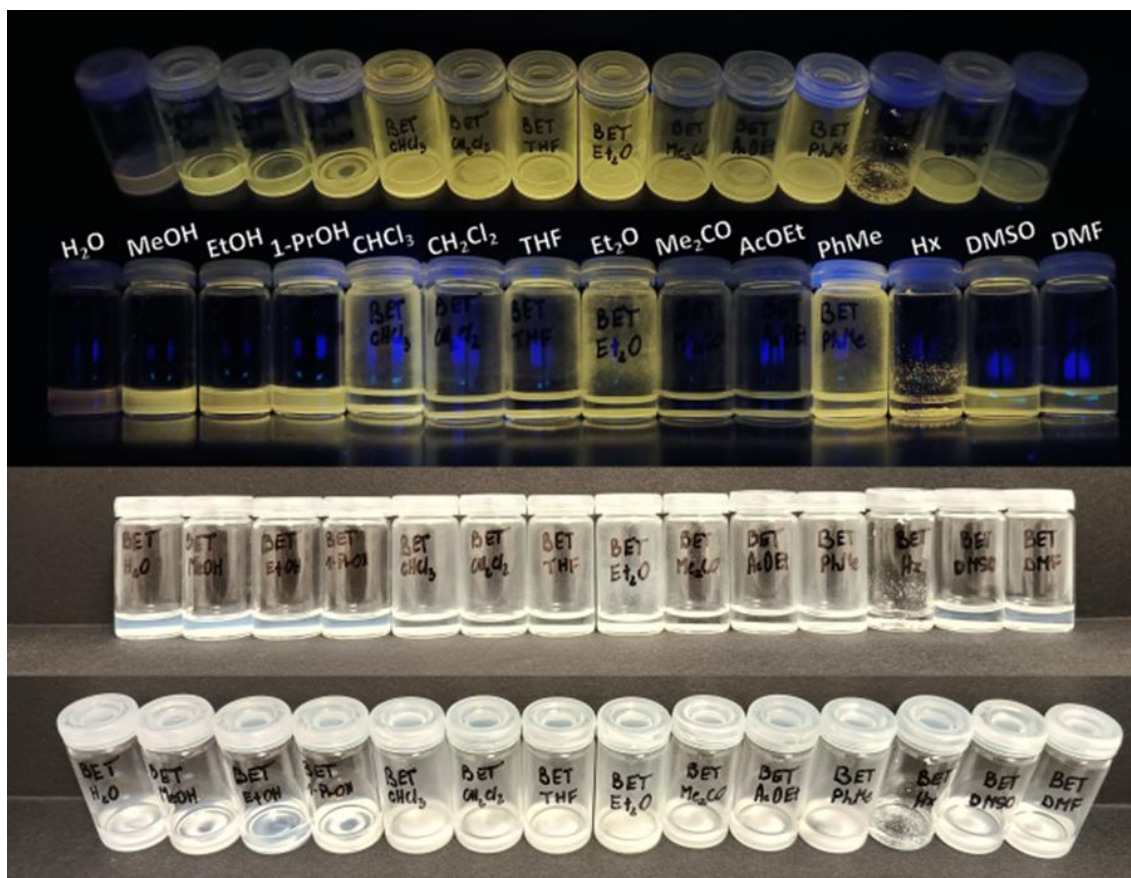


**Figure S9.** Photographs of ZnO-BET QDs dispersion under UV lamp light ( $\lambda_{ex} = 366$  nm) and visible light.

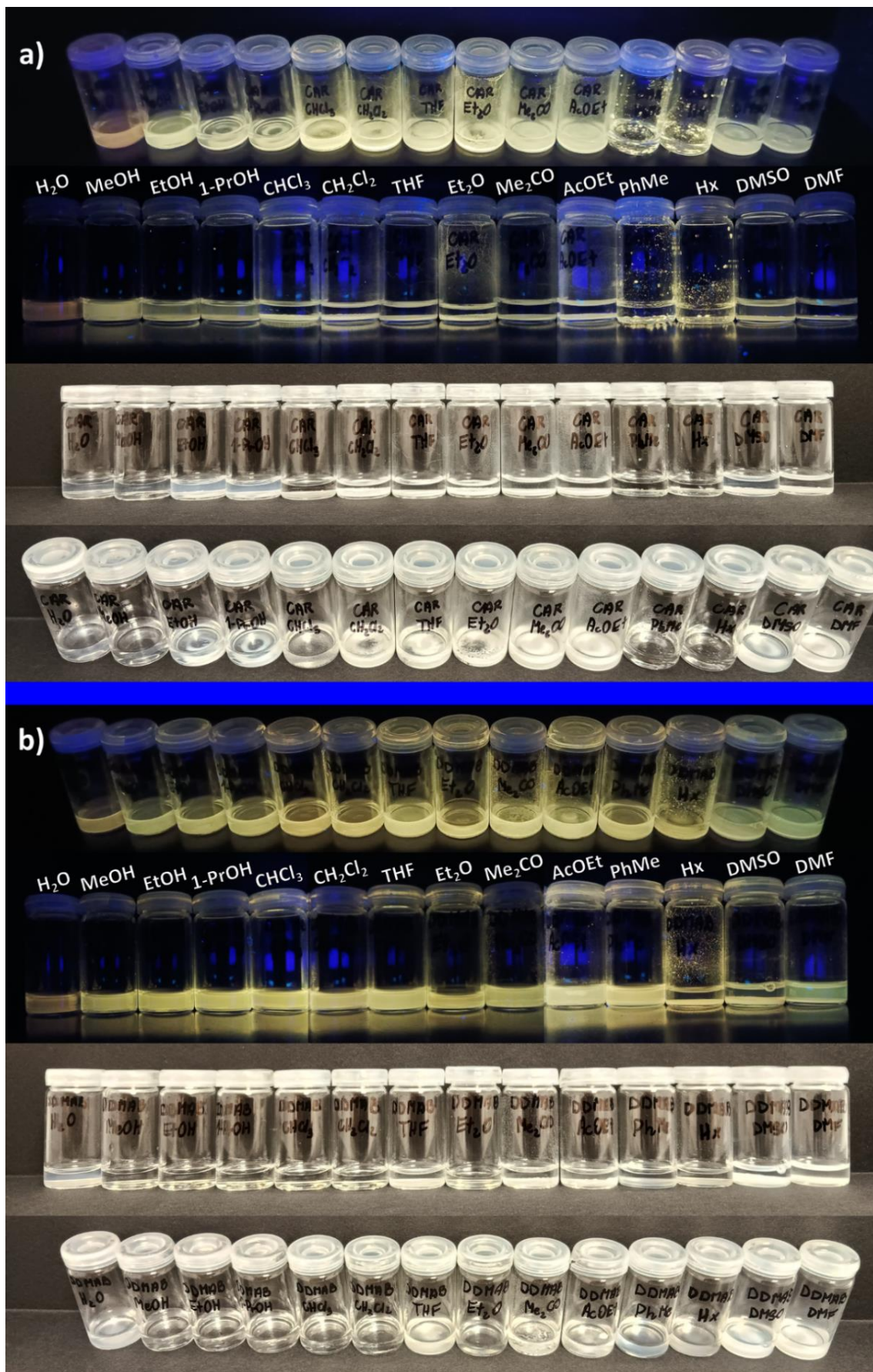


**Figure S10.** Photographs of dispersions of (a) ZnO-CAR and (b) ZnO-DDMAB QDs under UV lamp light ( $\lambda_{ex} = 366$  nm) and visible light.

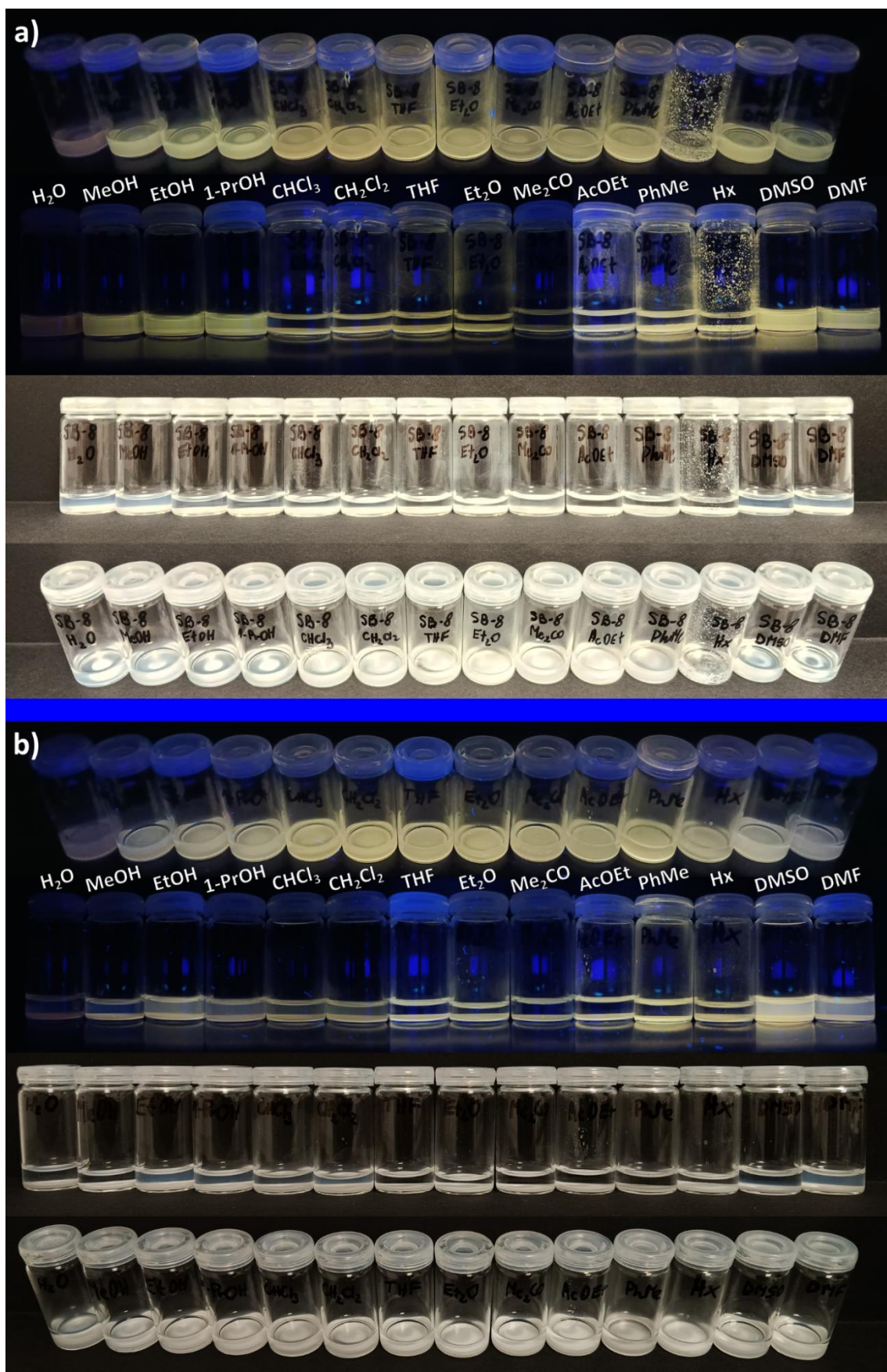


**Figure S11.** Photographs of dispersions of (a) ZnO-SB-8 and (b) ZnO-NDSB-201 QDs under UV lamp light ( $\lambda_{ex} = 366$  nm) and visible light.

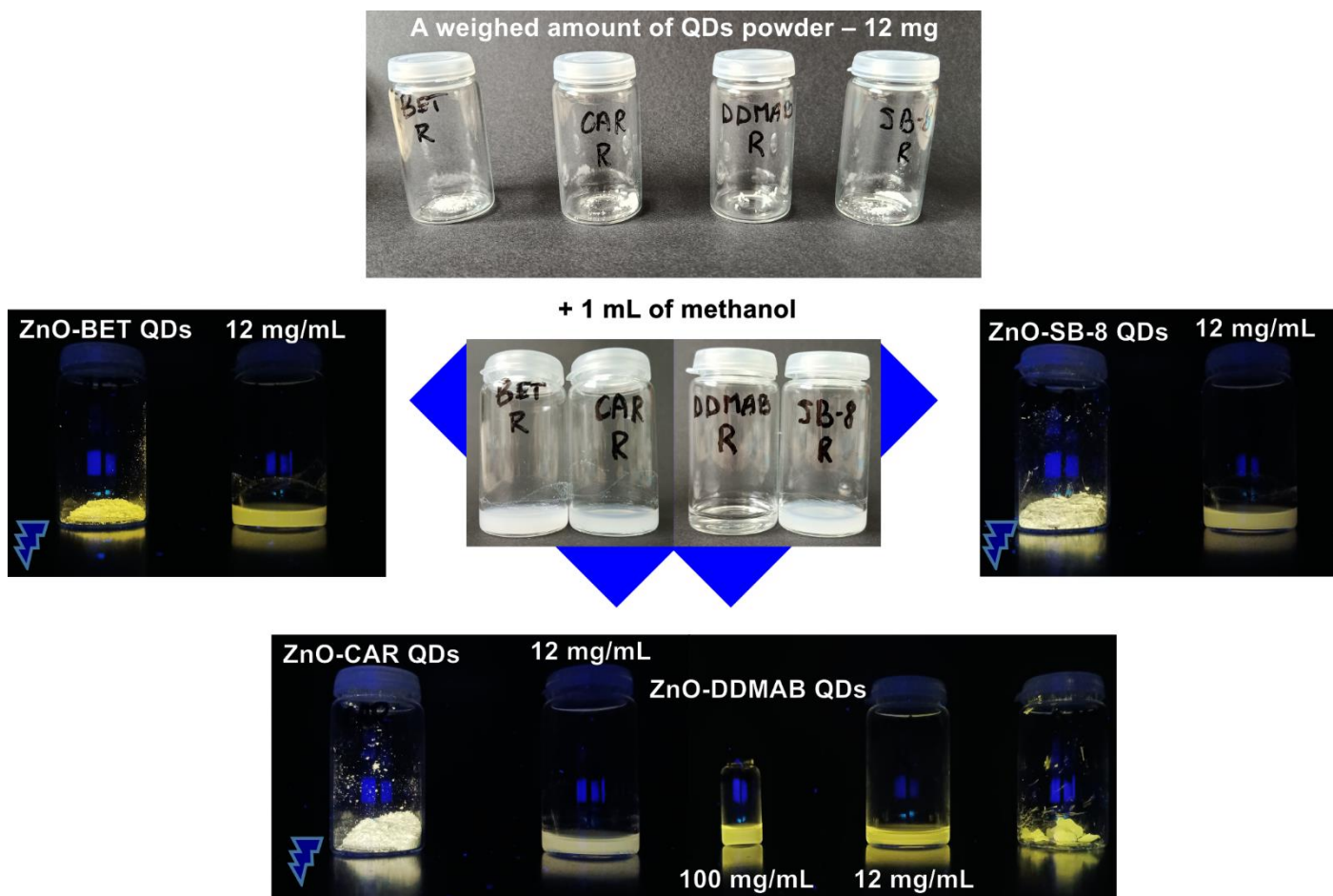


**Figure S12.** Images of ZnO QDs in solid form and methanol dispersions taken under visible or UV light illumination ( $\lambda_{\text{ex}} = 366$  nm).

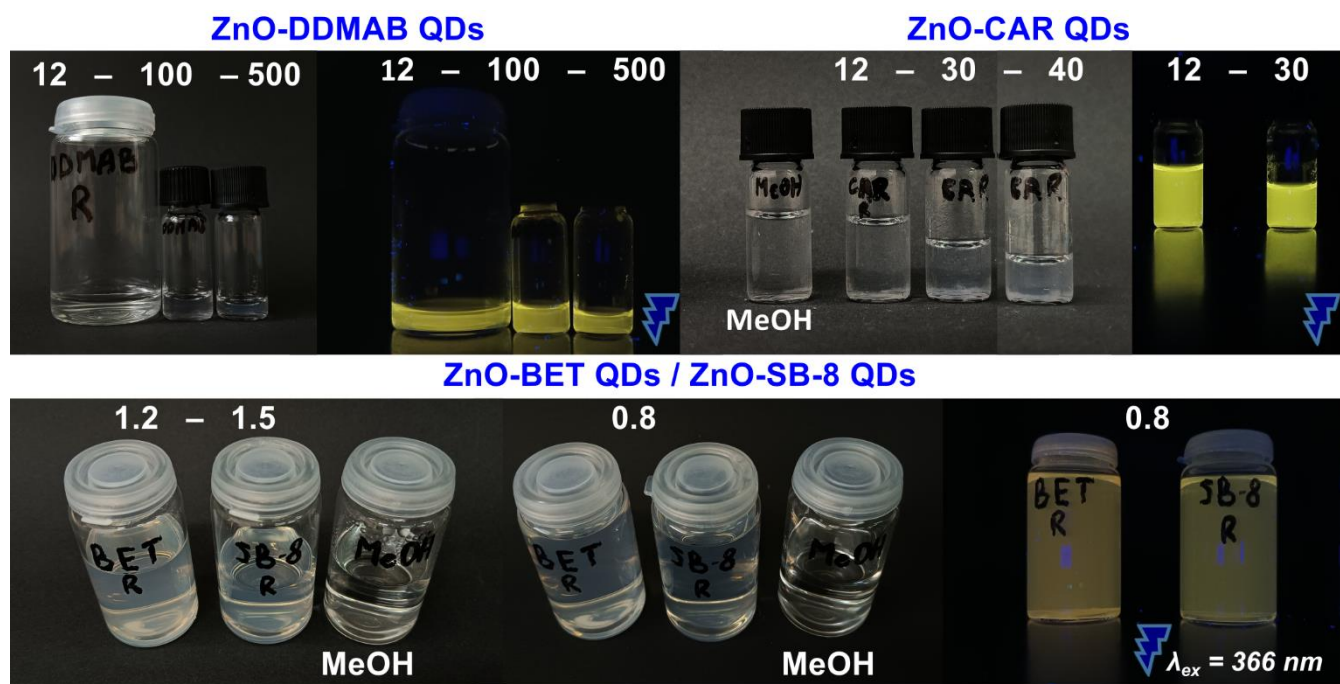


**Figure S13.** Colloidal dispersions of selected ZnO QDs in MeOH after approx. 12 hours of preparation (the QDs concentrations [mg/mL] are indicated accordingly).

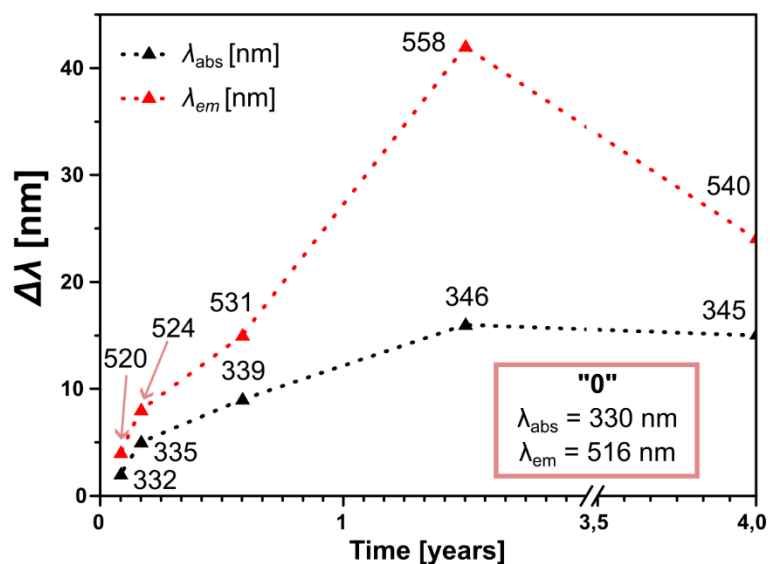


**Figure S14.** Bathochromic shifts in absorption and emission observed over a 4-year period for **ZnO-DDMAB QDs** dispersed in methanol, along with the corresponding  $\lambda_{abs}$  and  $\lambda_{em}$  values (initial values are shown in the graph).

## 2. Solution stability of ZnO QDs coated with carboxylate ligands

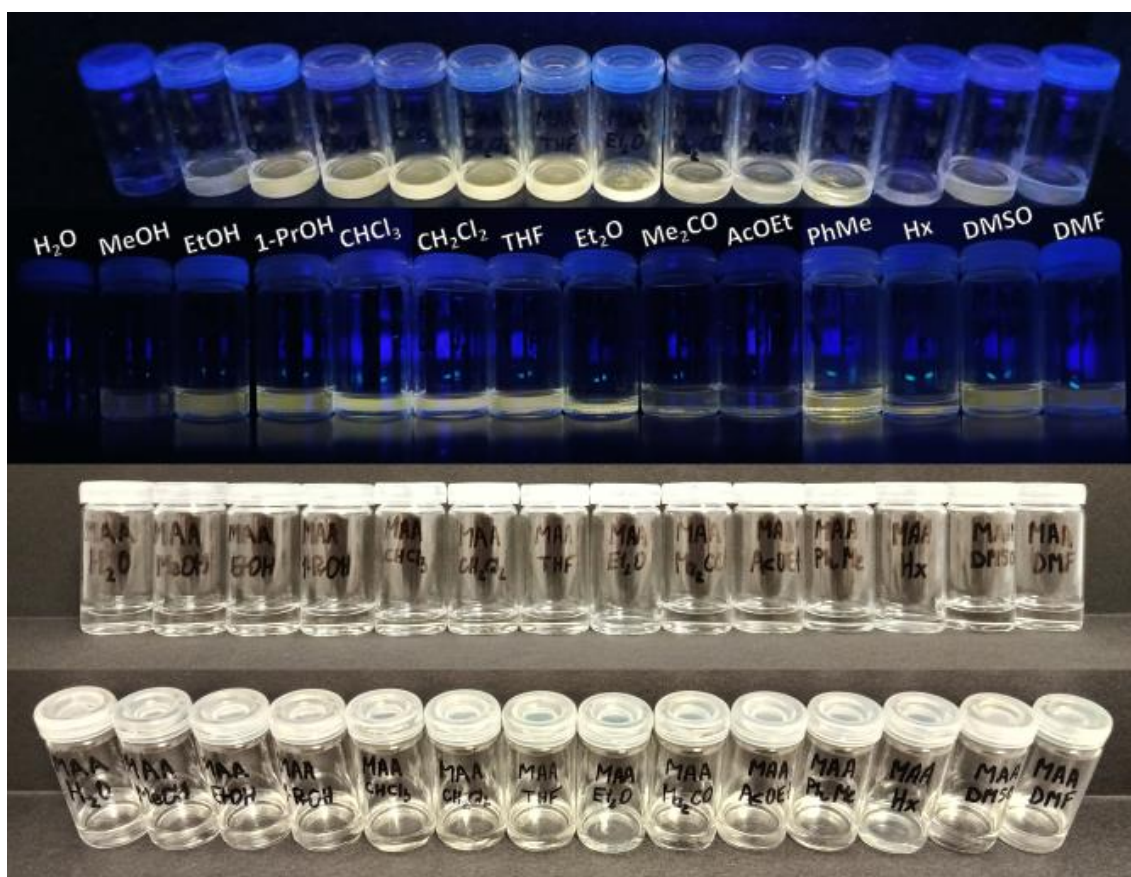


**Figure S15.** Photographs of **ZnO-MAA QDs** dispersion under UV lamp light ( $\lambda_{ex} = 366$  nm) and visible light.

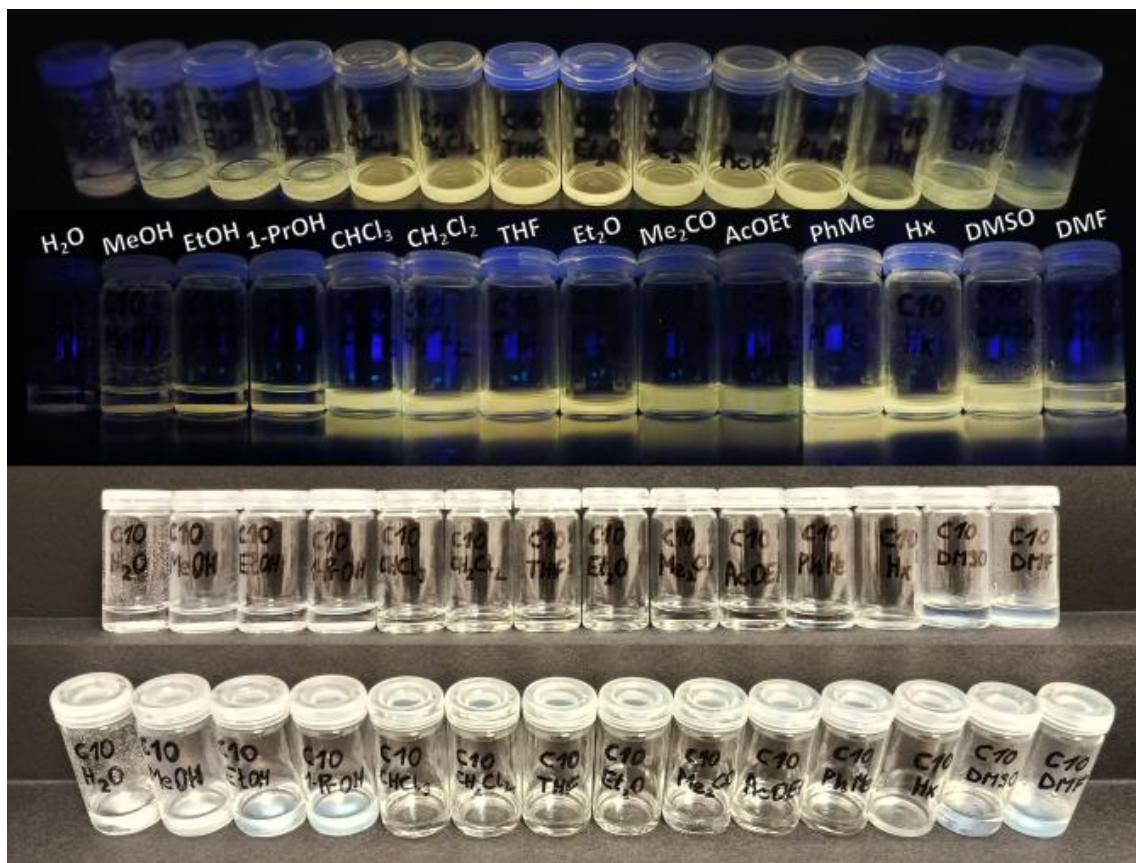


Figure S16. Photographs of ZnO-C10 QDs dispersion under UV lamp light ( $\lambda_{\text{ex}} = 366 \text{ nm}$ ) and visible light.

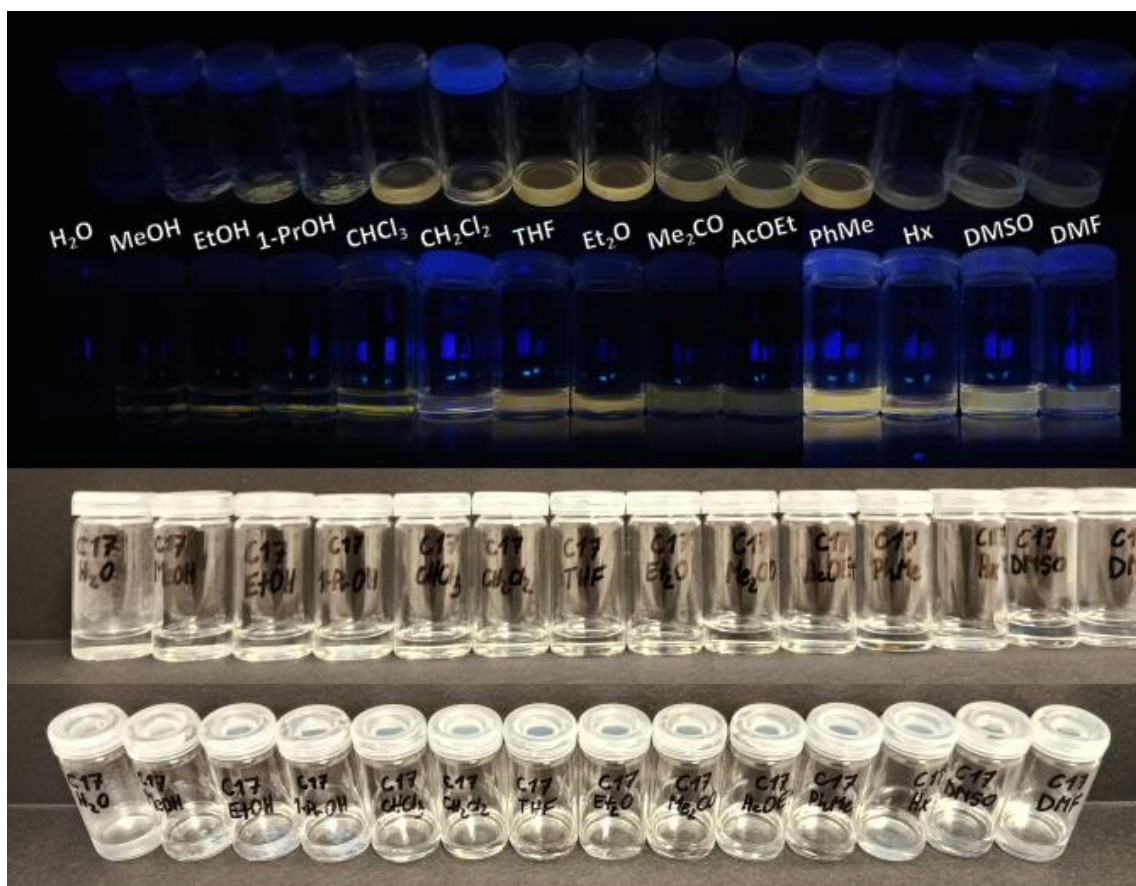
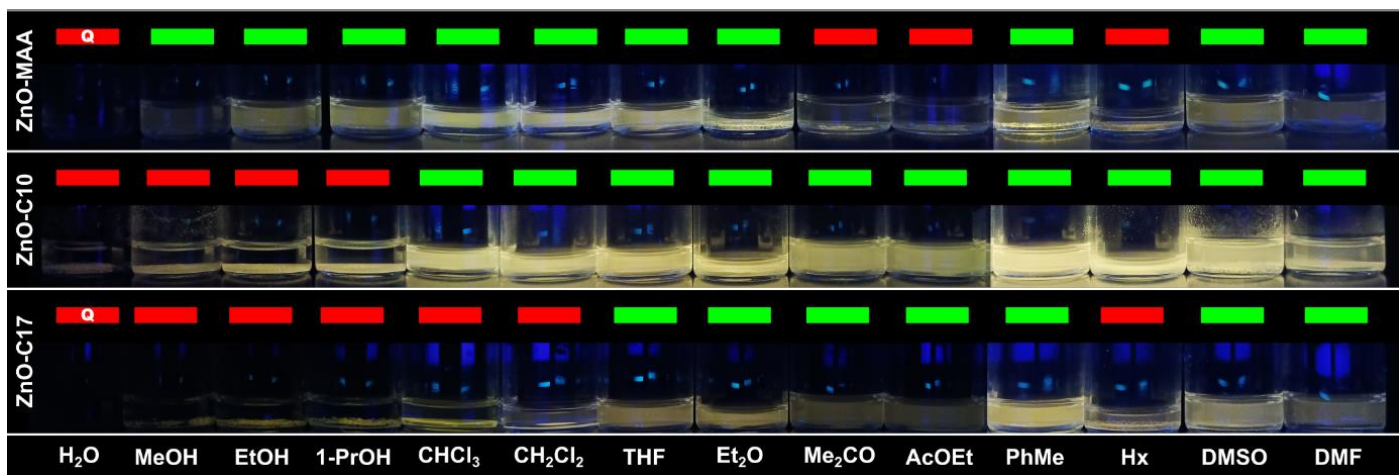
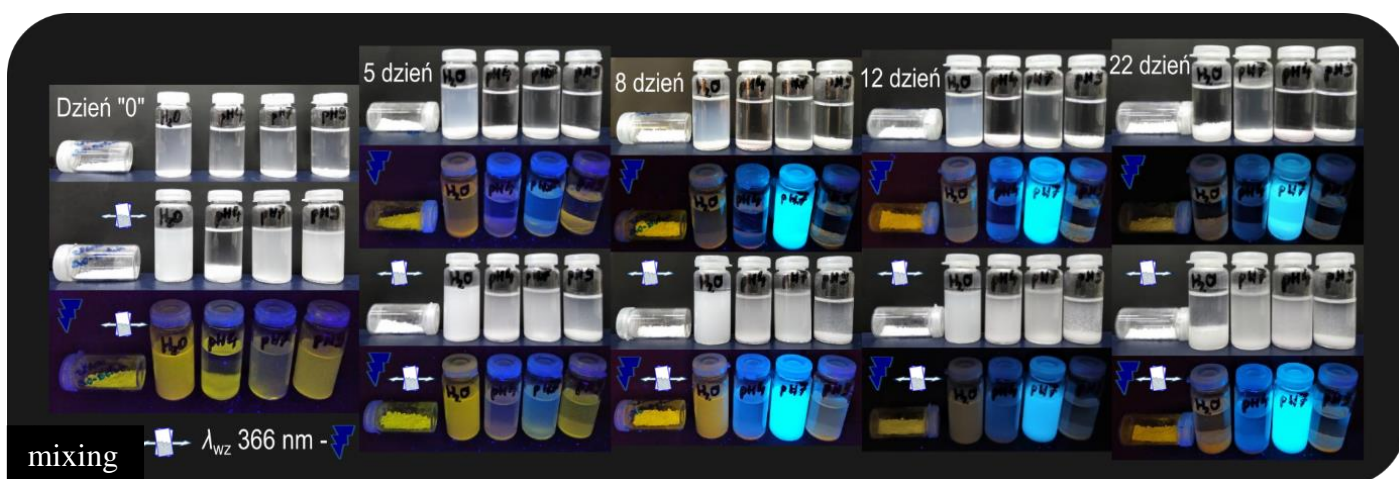


Figure S 17. Photographs of dispersions of ZnO-C17 QDs under UV lamp light ( $\lambda_{\text{ex}} = 366 \text{ nm}$ ) and visible light.



**Figure S18.** Ability of ZnO-MAA, ZnO-C10, and ZnO-C17 QDs to form long-term colloidal dispersion in selected solvents (green – stable colloidal solution, red – sedimenting; Q – PL quenching).

### 3. Effect of buffer pH and water on the colloidal stability and luminescence of ZnO-BET QDs



**Figure S19.** A compilation of images of ZnO-BET QDs dispersions in buffers (pH 4, pH 7, and pH 9) over 22 days.